

**SYNTHESIS AND CHARACTERIZATION OF
MAGNESIUM OXIDE NANOMATERIALS VIA
DIRECT HEATING METHOD**

KOK KAI LIN

UNIVERSITI SAINS MALAYSIA

2022

SCHOOL OF MATERIALS AND MINERAL RESOURCES ENGINEERING
UNIVERSITI SAINS MALAYSIA

SYNTHESIS AND CHARACTERIZATION OF MAGNESIUM OXIDE
NANOMATERIALS VIA DIRECT HEATING METHOD

by

KOK KAI LIN

Supervisor: Assoc. Prof. Ts. Ir. Dr. Pung Swee Yong

Dissertation submitted in partial fulfillment
of the requirements for the degree of Bachelor of Engineering with Honours
(Materials Engineering)

Universiti Sains Malaysia

AUGUST 2022

**SCHOOL OF MATERIALS AND MINERAL RESOURCES ENGINEERING
UNIVERSITI SAINS MALAYSIA**

**SYNTHESIS AND CHARACTERIZATION OF MAGNESIUM OXIDE
NANOMATERIALS VIA DIRECT HEATING METHOD**

By

KOK KAI LIN

Supervisor: Assoc. Prof. Ts. Ir. Dr. Pung Swee Yong

Dissertation submitted in partial fulfillment of the requirements for the degree of

Bachelor of Engineering with Honours

(Materials Engineering)

Universiti Sains Malaysia

AUGUST 2022

DECLARATION

I hereby declare that I have conducted, completed the research work and written the dissertation entitled '**Synthesis and Characterization of Magnesium Oxide Nanomaterials via Direct Heating Method**'. I also declare that it has not been previously submitted for the award of any degree and diploma or other similar title of this for any other examining body or University.

Name of Student: Kok Kai Lin

Signature:

Date: 12 AUGUST 2022

Witness by

Supervisor: Assoc. Prof. Ts. Ir. Dr. Pung

Signature:

Swee Yong

Date: 12 AUGUST 2022

ACKNOWLEDGMENT

First of all, I would like to express my appreciation to University Sains Malaysia and School of Materials and Mineral Resources for giving me this opportunity to carry out a Final Year Project, this has allowed me to gain a lot more experience and knowledge. This project would not be successful if without the school's facilities and equipment.

I express my sincere thanks to my final year project's supervisor, Assoc. Prof. Ts. Ir. Dr. Pung Swee Yong. His knowledge and guidance were superior, and this project would not be done without his support and advice.

I would like to thank my mother, Lau Kui Yong, who always ask about my progress and giving me unconditional love and support throughout this project. Nonetheless, I would like to thank my friends, Ng Guan Sheng and Liong Kai Ming, who always be in the same lab with me, which indirectly gave me support and companion.

TABLE OF CONTENT

DECLARATION	i
ACKNOWLEDGMENT	ii
TABLE OF CONTENT	iii
LIST OF FIGURES	vii
LIST OF TABLES	xi
LIST OF ABBREVIATION	xiv
LIST OF SYMBOLS	xv
ABSTRAK	xvii
ABSTRACT.....	xviii
CHAPTER 1 INTRODUCTION.....	1
1.1 Introduction	1
1.2 Nanotechnology and Nanomaterials	1
1.3 Problem statement.....	8
1.4 Research Objective.....	11
1.5 Scope of Study	11
1.6 Thesis Outline	12
CHAPTER 2 LITERATURE REVIEW.....	13
2.1 Introduction	13
2.2 Magnesium Oxide (MgO)	13
2.3 Synthesis methods of MgO nanomaterials.....	15

2.3.1	Sol-gel method	15
2.3.2	Ultrasonic method	17
2.3.3	Hydrothermal method	19
2.3.4	Green synthesis	21
2.3.5	Microwave-assisted method	22
2.3.6	Solid-state synthesis.....	24
2.4	Applications of MgO.....	29
2.5	Classification of Dye.....	30
2.5.1	Methylene Blue.....	31
2.6	MB dye removal methods	33
2.6.1	Advanced oxidation processes (AOPs).....	34
2.6.1 (a)	Photocatalysis	35
2.7	Scavenger tests	36
2.8	Degradation mechanism of MB dye and its degradation pathways	39
CHAPTER 3 METHODOLOGY		43
3.1	Introduction	43
3.2	Process flow	43
3.3	Materials and list	45
3.4	Synthesis of MgO nanomaterials via DH method.....	47
3.4.1	Experimental design	49
3.4.1 (a)	Effect of precursors	49
3.4.1 (b)	Effect of heating duration	50

3.4.1 (c) Effect of the power supply	50
3.5 Characterization methods	51
3.5.2 X-ray Diffraction (XRD)	53
3.5.3 Fourier transform infrared spectrometer (FTIR)	54
3.5.4 Transmission Electron Microscope (TEM)	54
3.5.5 Ultraviolet-visible (UV-Vis) spectrophotometer	55
3.5.6 Photocatalytic test - Methylene Blue dye removal using MgO nanomaterials	
56	
3.5.7 Scavenger test	58
CHAPTER 4 RESULTS AND DISCUSSION.....	59
4.1 Introduction	59
4.2 Synthesis and characterization of MgO nanomaterials grown on kanthal wires	
via DH method	59
4.2.1 Effect of types of precursors	59
4.2.1 (a) Structural properties	60
4.2.2 Effect of heating duration	67
4.2.2 (a) Structural properties	67
4.2.2 (b) Photocatalytic performances of MgO nanomaterials grown on kanthal	
wires 73	
4.2.3 Effect of heating power.....	79
4.2.3 (a) Structural properties	79

4.2.3 (b) The photocatalytic performance of MgO nanomaterials grown on kanthal wires	85
4.2.4 Characterization of MgO particles (by-product) synthesized with optimum parameters (45 min, 50 W)	90
4.2.4 (a) Structural properties	90
4.2.4 (b) The photocatalytic performance of MgO particles (by-product)	92
4.2.4 (c) Scavenger test for MgO particles (by-product)	96
CHAPTER 5 CONCLUSIONS AND RECOMMENDATIONS	101
5.1 Conclusions	101
5.2 Recommendations	102
REFERENCES.....	103
APPENDIX A.....	122

LIST OF FIGURES

Figure 2.1: Crystal structure of MgO (Smyth <i>et al.</i> , 2000).	14
Figure 2.2: Steps involved in the sol-gel method (Kallawar <i>et al.</i> , 2021).	16
Figure 2.3: SEM micrograph of MgO nanoparticles produced by Sutapa <i>et al.</i> (2018).	17
Figure 2.4: HRTEM micrograph of MgO nanomaterials formed by Gandhi <i>et al.</i> (2011).	18
Figure 2.5: SEM images of MgO nanoflakes produced by Dhal <i>et al.</i> (2015) observed under magnification of (a) 5,000 X and (b) 10,000 X.	20
Figure 2.6: (a) SEM (b) TEM micrograph of MgO nanoparticles synthesized using the microwave-assisted method by Mirzaei and Davoodnia (2012).	23
Figure 2.7: FESEM micrograph of MgO nanoparticles annealed for (a) 6 hr, (b) 12 hr, and (c) 24 hr formed by Kamarulzaman, Chayed, and Badar (2016).	25
Figure 2.8: Classification of dyes based on surface charge (Singh <i>et al.</i> , 2015).	31
Figure 2.9: Structural changes of MB upon oxidation and reduction (Khan <i>et al.</i> , 2022).	32
Figure 2.10: Number of articles in Scopus database which is related to MB dye removal or degradation (Data collected from Scopus by searching keywords “methylene AND blue OR dye OR removal OR degradation” on the date of April 7th, 2022).	33
Figure 2.11: Types of AOPs available that involve •OH as an oxidizing agent (Brugnera <i>et al.</i> , 2016).	35
Figure 2.12: Schematic diagram of MB degradation by MgO nanoparticle (Sackey <i>et al.</i> , 2020a).	41
Figure 2.13: Possible degradation pathways for MB dye with the presence of photocatalyst (Jia <i>et al.</i> , 2018).	42
Figure 3.1: Process flow chart of this project.	44

Figure 3.2: (a) Length, (b) leads, and (c) diameter of kanthal wires.	47
Figure 3.3: Experimental setup for DH method to produce MgO nanomaterials.....	48
Figure 3.4: Schematic diagram of DH method for MgO nanomaterials synthesis.	48
Figure 4.1: SEM images of the deposits on the kanthal wires with different types of precursors : (a,b) Bare wire; (c,d) Type 1; (e,f) Type 2; and (g,h) Type 3 at x120 and x500 magnification, respectively.	61
Figure 4.2: SEM images of deposits on kanthal wire synthesized using Type 3 precursor by DH method (a) 5,000 X, (b) 30,000 X and (c) EDX spectra.	62
Figure 4.3: XRD plots of (a) bare kanthal wire; and (b) nanomaterials grown on kanthal wire using Type 3 precursor (50 W, 60 min).....	63
Figure 4.4: XRD plots of particles (by-product) synthesized by DH method using Type 3 precursor at 50 W for 60 min.	64
Figure 4.5: FTIR spectral for (a) bare kanthal wire, (b) MgO nanomaterials deposited on the surface of kanthal wire. (The spectral range increased from 400-4000 cm^{-1} to 100-4000 cm^{-1} due to no signals observed in the previous range.)	65
Figure 4.6: FTIR spectral for MgO particles (by-product).....	67
Figure 4.7: SEM images for (a) 0 (bare kanthal wire), (b) 5, (c) 15, (d) 30, (e) 45, and (f) 60 min at 30,000X magnification.	69
Figure 4.8: XRD plots of particles (by-product) synthesized by DH method using Type 3 precursor at 50 W of heating power and (a) 5, (b) 15, (c) 30, (d) 45 and (e) 60 min.	71
Figure 4.9: FTIR spectra of MgO nanomaterials synthesized by DH using Type 3 precursor at 50 W of heating power and (a) 5, (b) 15, (c) 30, (d) 45 and (e) 60 min.	72
Figure 4.10: Absorbance spectra of MB solution degraded by MgO nanomaterials synthesized by DH using Type 3 precursor at 50 W of heating power and (a) 5, (b) 15, (c) 30, (d) 45 and (e) 60 min.	74

Figure 4.11: Removal efficiency of MB by MgO nanomaterials synthesized on kanthal wires at different heating duration.	75
Figure 4.12 : Kinetic plots of (a) Pseudo-zero-order, (b) Pseudo-first-order, (c) Pseudo-second-order kinetics; and (d) rate constants for photocatalytic degradation of MB by MgO nanomaterials grown on kanthal wires synthesized at different heating duration.	77
Figure 4.13: SEM images for MgO nanomaterials grown on the surface of kanthal wires by DH method using (a) 0, (b) 10, (c) 20, (d) 30, (e) 40, and (f) 50 W at 50,000 X.	81
Figure 4.14: XRD plot of MgO and Mg(OH) ₂ for (a) 10, (b) 20, (c) 30, (d) 40, and (e) 50 W of heating power.....	83
Figure 4.15: FTIR spectra for MgO nanomaterials at: (a) 10, (b) 20, (c) 30, (d) 40, and (e) 50 W of heating power.....	84
Figure 4.16: Absorbance spectra of MB solution degraded by MgO nanomaterials synthesized by DH at (a) 10, (b) 20, (c) 30, (d) 40, and (e) 50 W of heating power.....	86
Figure 4.17 : Removal efficiency of MB by MgO nanomaterials synthesized on kanthal wires at different heating power.	87
Figure 4.18: Kinetic plots of (a) Pseudo-zero-order, (b) Pseudo-first-order, (c) Pseudo-second-order kinetics; and (d) rate constants for photocatalytic degradation of MB by MgO nanomaterials grown on kanthal wires synthesized at different heating duration.	89
Figure 4.19: XRD plots of (a) commercial MgO powder and (b) MgO particles (by-product) synthesized by DH method with optimum parameters (45 min, 50 W).....	91
Figure 4.20: FTIR spectra for (a) commercial MgO powder, (b) MgO particles (by-product).....	92
Figure 4.21: Absorbance spectra of MB solution degraded by (a) commercial MgO powder, (b) MgO particles (by-product).....	93

Figure 4.22: Removal efficiency of MB by commercial MgO powder and MgO particles (by-product).	94
Figure 4.23: (a) UV-Vis absorption spectrum and (b) Band gap spectra for the by-product of synthesized MgO nanomaterials.....	95
Figure 4.24: Absorbance spectra of MB solution degraded by MgO particle (by-product) synthesized with optimum parameters (a) without scavenger, (b) EDTA, (c) H ₂ O ₂ , (d) IPA, and (e) BQ.	97
Figure 4.25: Removal efficiency of MB by MgO particles (by-product) with the addition of different scavengers.....	98
Figure 4.26: TEM morphology of the synthesized nanomaterials on the surface of kanthal wire at (a) 9,900X, (b) 38,000X, (c) 43,000X, (d) 97,000X (focus of c), (e) 1,500,000X (focus of d).....	100
Figure 5.1: River water quality from the year 2008 to 2017 in Malaysia (Lee Goi, 2020).	122
Figure 5.2: River water quality from the year 2008 to 2017 according to states in Malaysia (Lee Goi, 2020).....	122

LIST OF TABLES

Table 1.1: Summary of advantages, disadvantages, and examples for top-down and bottom-up approaches.....	4
Table 2.1: Synthesis parameters, advantages, and disadvantages of different synthesis methods.....	27
Table 2.2: Synthesis parameters, advantages, and disadvantages of different synthesis methods (cont.).....	28
Table 3.1: List of materials used.....	45
Table 3.2: List of materials used in this study (cont.).....	46
Table 3.3: Chemicals used to produce the Type 1, Type 2, and Type 3 precursor solutions.....	49
Table 3.4: Synthesis parameters used to study the effect of heating duration on the growth of MgO nanomaterials	50
Table 3.5: Synthesis parameters used to study the effect of heating duration on the growth of MgO nanomaterials	51
Table 4.1: Quantitative analysis for surface coverage of deposits on the surface of kanthal wires via ImageJ software based on Figure 4.1 (d), (f) and (h).....	62
Table 4.2: Riveted refinement for the XRD plot of MgO and Mg(OH) ₂ for content estimation in particles (by-product) synthesized by DH method using Type 3 precursor at 50 W, 60 min.	65
Table 4.3: Quantitative analysis for diameter and length of deposits on the surface of kanthal wires via ImageJ software based on Figure 4.7.	70
Table 4.4: Surface coverage analysis of deposited MgO nanomaterials at different heating duration via ImageJ software based on Figure 4.7.	70

Table 4.5: Riveted refinement for the XRD plot of MgO and Mg(OH) ₂ for content estimation in particles (by-product) synthesized by DH method using Type 3 precursor at 50 W for different heating durations.....	71
Table 4.6: Removal efficiencies of MgO nanomaterials grown on kanthal wire at different heating duration.	75
Table 4.7: Kinetic parameters for removal efficiency of MB with MgO nanomaterials deposited on kanthal wire.	78
Table 4.8: Photocatalytic performances of MgO nanomaterials synthesized using Type 3 precursor at 50 W for 45 min.....	78
Table 4.9: Temperature for different heating power after heating for 45 min.....	79
Table 4.10: Summary of structures grown on kanthal wire using different synthesis parameters.....	80
Table 4.11: Surface coverage analysis of deposited MgO nanomaterials at different heating power via ImageJ software based on Figure 4.13.....	82
Table 4.12: Riveted refinement for the XRD plot of MgO and Mg(OH) ₂ for content estimation in the particles (by-product) synthesized at different heating power using Type 3 precursor at 45 mins.....	83
Table 4.13: Removal efficiencies of MgO nanomaterials grown on kanthal wire at different heating power.....	87
Table 4.14: Kinetic parameters for removal efficiency of MB with MgO nanomaterials deposited on kanthal wire.	89
Table 4.15: Riveted refinement for the XRD plot of MgO and Mg(OH) ₂ for content estimation in the commercial MgO powder, and MgO particles (by-product) synthesized by DH method using Type 3 precursor at 50 W for different heating durations.....	90

Table 4.16: Removal efficiencies of MgO nanomaterials grown on kanthal wire at different heating power.	92
Table 4.17: Removal efficiencies of MgO particles (by-product) with the addition of scavengers.	98
Table 4.18: Measurements of different morphology based on Figure 4.26 (b).	99

LIST OF ABBREVIATION

AOPs	Advanced Oxidation Processes
BQ	1,4- Benzoquinone
DH	Direct Heating
Doe	Department of Environment
EDX	Energy Dispersive X-Ray
FESEM	Field Emission Scanning Electron Microscope
FTIR	Fourier Transform Infrared
IPA	Isopropyl Alcohol
MB	Methylene Blue
OFAT	One-Factor-at-a-Time
TEM	Transmission Electron Microscope
Tiron	Sodium 4,5- Dihydroxybenzene-1,3-Disulfonate
UV-Vis	Ultraviolet–Visible
XRD	X-Ray Diffraction

LIST OF SYMBOLS

α	Absorption Coefficient
α_0	Absorption Edge Width Parameter
θ	Angle
E_g	Band Gap
cm	Centimetre
C	Concentration
C_0	Concentration At Time = 0
°	Degree
°C	Degree Celsius
e^-	Electron
n	Exponent
g	Gram
g/mol	Gram Per Mole
Hz	Hertz
h^+	Hole
h^+	Hole

hr	Hour
•OH	Hydroxyl Radicals
hν	Incident Photon Energy
λ	Lambda, Wavelength
μm	Micrometre
mgL ⁻¹	Milligram Per Liter
mL	Millilitre
mm	Millimetre
mM	Millimolar
min	Minute
nm	Nanometre
%	Percentage
%T	Transmittance
V	Volt
W	Watt
Pm(mT) ⁻¹	Sensitivity

**SINTESIS DAN PENCIRIAN BAHAN NANO MAGNESIUM OKSIDA
DIDEPPOSIT MELALUI CARA PEMANASAN LANGSUNG
ABSTRAK**

Memandangkan bahan nano menjadi suatu semakin penting dalam kehidupan seharian, pelbagai jenis kaedah sintesis telah diciptakan untuk menghasilkan bahan nano dengan rupa luaran (atau morfologi) dan ciri yang berbeza. Bahan nano oksida logam telah menjadi salah satu bahan yang menarik untuk disintesis untuk kegunaan fotodegradasi. Hal ini disebabkan masalah pencemaran alam sekitar yang semakin serius, menyebabkan kebangkitan applikasi ini. Bahan nano magnesium oksida (MgO) adalah salah satu bahan yang boleh digunakan sebagai pemangkin foto. Projek ini bertujuan untuk mencipta bahan nano MgO melalui kaedah Pemanasan Langsung yang baru dibangunkan pada permukaan dawai kanthal yang bertindak sebagai sentuhan kuat untuk mengelakkan bahan dikupas semasa proses fotodegradasi. Projek ini mengkaji kesan jenis prekursor iaitu $\text{Mg}(\text{NO}_3)_2$, PEG 200, NH_3 (Jenis 1), MgCl_2 , NaOH (Jenis 2) dan $\text{Mg}(\text{NO}_3)_2$, NaOH (Jenis 3), pemanasan tempoh (iaitu 0, 5, 15, 30, 45, dan 60 min) dan kuasa pemanasan (iaitu 0, 10, 20, 30, 40, 50 W) untuk pertumbuhan bahan nano MgO pada permukaan dawai kanthal. XRD, FTIR, dan TEM membuktikan bahan nano MgO telah berjaya dicipta, menunjukkan kejayaan membangunkan kaedah Pemanasan Langsung untuk mensintesis bahan nano MgO. Keadaan sintesis yang digunakan untuk menghasilkan bahan nano MgO adalah dengan menggunakan prekursor Jenis 3 dan kuasa pemanasan 50 W selama 45 minit. Keadaan sintesis tersebut telah menghasilkan batang nano MgO (diameter ~ 74.97 nm, panjang ~ 184.98 nm), liputan permukaan ke atas permukaan dawai kanthal yang baik (92.05%). Kecekapan fotodegradasi batang nano MgO ini di bawah penyinaran UV ialah 34.53%.

SYNTHESIS AND CHARACTERIZATION OF MAGNESIUM OXIDE NANOMATERIALS VIA DIRECT HEATING METHOD

ABSTRACT

As nanomaterials become increasingly inevitable in everyday life applications, various kinds of synthesis methods have been developed to produce nanomaterials with different morphologies and characteristics. Metal oxides nanomaterials have been one of the attractive materials to be synthesized for the application of photodegradation, due to the severe environmental pollution in recent years. MgO nanomaterials are one of the promising materials that can be used as photocatalysts. This project aims to synthesize MgO nanomaterials via the newly developed Direct Heating (DH) method on the surface of the kanthal wire that provide certain support to avoid massive loss of nanomaterials during application for instance wastewater treatment process. This project studied the effects of types of precursors i.e. $\text{Mg}(\text{NO}_3)_2$, PEG 200, NH_3 (Type 1), MgCl_2 , NaOH (Type 2) and $\text{Mg}(\text{NO}_3)_2$, NaOH (Type 3), heating duration (i.e. 0, 5, 15, 30, 45, and 60 min) and heating power (i.e. 0, 10, 20, 30, 40, 50 W) for the growth of MgO nanomaterials on kanthal wires. The XRD, FTIR, and TEM proved the presence of MgO nanomaterials, indicating the success of developing the DH method to synthesize MgO nanomaterials. The optimized synthesis condition to produce MgO nanomaterials was using Type 3 precursor and 50 W heating power for 45 min. This was because this synthesis condition produced MgO nanorods (diameter ~ 74.97 nm, length of ~ 184.98 nm), and good surface coverage (92.05%). The photodegradation efficiency of these MgO nanorods under UV irradiation was 34.53%.

CHAPTER 1 INTRODUCTION

1.1 Introduction

This chapter presents the research background of this project, providing the rationale for the needs to develop a simple, yet time- and cost-effective direct heating (DH) method for the growth of Magnesium Oxide (MgO) photocatalyst on kanthal wires. The problems associated with the development of the DH method and deterioration of photocatalytic performance over time due to the loss of photocatalyst in particle form are discussed. Subsequently, the research objectives and scope of the project are presented. Lastly, the layout of this thesis is briefly presented.

1.2 Nanotechnology and Nanomaterials

According to ISO/TS 80004-1:2015, nanotechnology is meant by the application of scientific knowledge to manipulate, control, and synthesis of materials with size in the nanoscale (approximately from 1 nm to 100 nm), and to make use of their properties in this particular size range which possesses different properties as compared to their properties when in bulk. In general, nanotechnology is a broad term that comprises science, research, engineering, and technology that involves materials that are on the nanoscale.

Nanotechnology has brought numerous prospective and significant benefits to the human being in various areas including human health (Sahoo *et al.*, 2007; Cattaneo *et al.*, 2010), device development (Ansari *et al.*, 2014), communication (Hao *et al.*, 2020), remediation of environmental pollution (Roy *et al.*, 2021; Darwesh *et al.*, 2022), environmental sensors (Kumar *et al.*, 2020) and renewable energy capture (Kumaş *et al.*, 2020). Figure 1.1 shows the nanotechnology and nanomaterials market share by

applications in the year 2020. As reported by Allied Market Research, the market size of nanotechnology on a worldwide scale was at \$1.76 billion in the year 2020 and was expected to reach \$33.63 billion by the year 2030 with a compound annual growth rate (CAGR) of 36.4%.

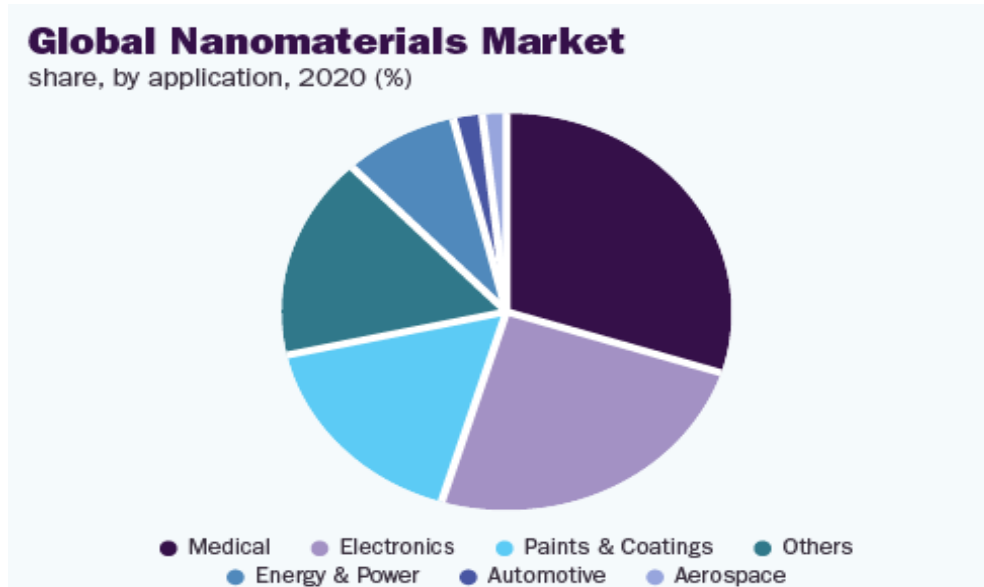


Figure 1.1: Nanotechnology and nanomaterials market share by applications in the year of 2020 (Grand View Research, 2021).

Nanomaterials are the materials that have dimensions within the nanoscale (less than 100 nm) and can be categorized based on their dimensionality (0-dimensional, 1-dimensional, 2-dimensional, or 3-dimensional); morphological nature (nanospheres, clusters, nanotube, nanowires, nanorods, thin films, plates or polycrystals); origin (natural or anthropogenic); chemical composition (inorganic, organic, single constituent, composites, metal oxide, polymeric or semiconductor); and formation (anthropogenic, geogenic or atmospheric) (Saleh *et al.*, 2016; Saleh, 2020).

Various synthesis methods have been developed to produce nanomaterials. The synthesis of nanomaterials is one of the key stages for the development of nanotechnology. This is due to the fact that synthesis methods will affect the structure, morphology, and

characteristics of nanomaterials, which leads to properties changes in the final products. In general, the synthesis of nanomaterials could be classified as top-down and bottom-up approaches. Table 1.1 shows the summary of advantages, disadvantages, and examples of synthesis methods for top-down and bottom-up approaches. Top-down approaches utilize mechanical methods to scale down a bulk material into nano-sized material while bottom-up approaches rely on atoms or molecules for self-assembly to produce nano-sized materials. The advantages of the top-down approaches are they are relatively low cost as compared to bottom-up approaches and have a simple procedure that commonly does not use any solvent. Nevertheless, the top-down approach has difficulty maintaining a constant shape and narrow size distribution as it utilizes mechanical force that will cause deformation of the material. For some of the top-down approaches, it might cause contamination of the nanomaterials due to the usage of equipment such as the miller. Bottom-up approaches, on the other hand, can produce the precise and smaller size of nanomaterials with narrow size distribution. It produces a relatively high purity of products, but the cost of equipment and raw materials are relatively higher, and the procedure can be complex with more parameters to control.

Table 1.1: Summary of advantages, disadvantages, and examples for top-down and bottom-up approaches.

	Top-Down	Bottom-up
Advantages	<ul style="list-style-type: none"> • Low cost • Simple process • High Productivity • Can have a solvent-less process 	<ul style="list-style-type: none"> • High purity product • Narrow size distribution • Can produce small size product • Precise control of size and shape
Disadvantages	<ul style="list-style-type: none"> • Low Purity • Broad size distribution • Inconsistent morphology 	<ul style="list-style-type: none"> • High equipment cost • Require precise control of synthesis parameters
Examples	<ul style="list-style-type: none"> • Ball milling • Thermal evaporation • Laser Ablation • Sputtering • Pulsed electrochemical etching 	<ul style="list-style-type: none"> • Chemical vapour deposition • Co-precipitation • Sol-Gel • Hydrothermal • Template-assisted • Flame spraying
Reference	(Meischein <i>et al.</i> , 2021; Sherif El-Eskandarany <i>et al.</i> , 2021; Abid <i>et al.</i> , 2022)	(Ayuk <i>et al.</i> , 2017)(Khan <i>et al.</i> , 2019)

In the past two decades, a significant amount of researches related to synthesizing, characterization, and development of their applications of metal oxide nanomaterials have been done due to their distinct behaviour which is entirely different from their bulk counterpart. These different behaviours can be explained by the possible quantum effects at the nanoscale and their high surface area to volume ratio, which changes the chemical and physical properties of these materials significantly (Guisbiers *et al.*, 2012). Metal oxide nanomaterials such as MgO (S.Lidvin *et al.*, 2015), ZnO (Srivastava *et al.*, 2013), CuO (Maruthupandy *et al.*, 2017), and SnO (Janardhan *et al.*, 2018) are synthesized by

the reaction between metallic materials and oxygen. These metal oxide nanomaterials are well suited for sensors (Yoon *et al.*, 2022), bio-imaging detectors (Anderson *et al.*, 2019), optical devices (Taeño *et al.*, 2021), antibacterial (Podder *et al.*, 2018), and wastewater (Sadri Moghaddam *et al.*, 2010) applications due to the following characteristics:

- (i) have cations with valence states and anions with deficiencies, and
- (ii) involve carriers depletion (Gangwar *et al.*, 2016).

Water pollution had become increasingly serious day by day and this will pose a serious threat to humans. In the year 2018, the Department of Environment (DoE) reported that out of 477 rivers, there were 51 rivers were categorized as polluted and 25 rivers of them were considered dead rivers (Yaseen *et al.*, 2019). The number of polluted rivers increased to 53% in the year 2020. In the year 2021, DoE has reported that 27.8% of the monitored river is not in the clean categories, where 33 river basins were categorized as moderately polluted, and 7 river basins were in the heavily contaminated category. Most of the polluted rivers came from the states with a high number of industrial areas for instance Penang and Johor as displayed in Figure 5.2 in Appendix A. It also stated that the major cause of river water pollution is pollutants discharged from the industrial area. Amongst them, the textile industries are the major ones responsible for toxic dye effluents.

The textile industry in Malaysia contributed RM 7.462 billion in the year 2021 with 10.09% of the increment (Malaysian Knitting Manufacturers Association, 2021). This indirectly indicates that this industry utilizes tons of dyes, and thus the volume of industrial effluents discharged from the textile industry will be huge in volume (Abu Bakar *et al.*, 2020). In addition, the Batik industry plays a vital role in the textile industry as it is recognized as a heritage of the country and has also contributed to the national

revenue (Mohamad Akhir *et al.*, 2017). In the year 2019, the Malaysian craft industry has a total revenue of RM 465.5 million with 34% of them coming from batik products based on about 320 batik producers that were registered under Malaysia Handicraft (Nordin *et al.*, 2012; ERDA, 2020). There is still a number of local batik producers that did not register under Malaysia Handicraft as they are afraid of losing their brand and design control, which leads to the actual revenue of batik products remaining unknown (Nita Jay, 2019).

Unfortunately, the contribution of economic growth for this product did not synchronize with their wastewater treatment system. Most of the batik producers in Malaysia are categorized as small-medium enterprises (SMEs) which usually have a low operating cost. Their production sites were thus built in their home backyard or nearby river side. As batik production utilizes a large amount of water, it is relatively convenient for them to discharge these high amounts of effluents into the river without proper treatment (Noor Syuhadah Subki *et al.*, 2011). Thus, wastewater treatment will be needed to avoid bringing adverse health effects to the environment and humans.

Wastewater treatment techniques such as using a membrane (Thamaraiselvan *et al.*, 2015; Ezugbe *et al.*, 2020; Kallawar *et al.*, 2021) and activated carbon (Kumbasar *et al.*, 2016; Jiang *et al.*, 2019; Kuang *et al.*, 2020) are common ways to remove organic dyes from wastewater. However, these techniques are costly particularly for small size Batik factories. Furthermore, the organic dyes trapped in the membranes and activated carbon are secondary pollutants that need further treatments. This will incur more cost and time.

Currently, numerous research had been done on the metal oxide nanomaterials as photocatalysts for environmental remediation, especially for water pollution (Nagajyothi *et al.*, 2020; Tahir *et al.*, 2020; Danish *et al.*, 2021). Photocatalysts using semiconductor

materials is one of the complementary techniques for the degradation of organic pollutants such as dyes in the effluents as it has high reactivity, high availability, convenience, and does not produce secondary pollutants after degradation (Alkaykh *et al.*, 2020). The photocatalytic oxidation process involves three steps in general. First, the organic pollutants will be absorbed onto the photocatalyst surface and interact. The mechanism of adsorption involves surface diffusion of the pollutants, followed by mass transfer between solid and liquid phase, then adsorption of pollutants to catalyst surface, and lastly diffusion of the adsorbed molecules through the catalyst pores (Andronic *et al.*, 2020). Next, photo-induced electrons and holes will be produced in the photocatalyst for redox reaction (Mahmood *et al.*, 2020). The third step involves by-product desorption from the surface of the photocatalyst.

Amongst all the available adsorbent materials, metal oxides are the most preferred due to their cost-effectiveness, and they can be synthesized easily (Li, 2019). MgO-based photocatalyst is said to be suitable for dye degradation as they have a low refractive index and a high surface area that improves the dye adsorption ability (Allawi *et al.*, 2020). As compared to TiO₂ (Pawar *et al.*, 2018) and ZnO (Mirzaeifard *et al.*, 2020), MgO-based photocatalyst is also preferable due to its high availability and low cost (Tahir *et al.*, 2020). For example, 1 kg of TiO₂ particles is RM 1309 but one kilogram of MgO only costs RM 832.50 (MkNANO, 2022). Reports show that nano-sized MgO has an appreciable efficiency as a photocatalyst (Bdewi *et al.*, 2015; Venkata Ratnam *et al.*, 2019; Y. Zheng *et al.*, 2019; Taourati *et al.*, 2020; Kumar *et al.*, 2022).

Every new synthesis method will open an opportunity to improve the quality of nanomaterials used in particular applications. For instance, plant-based or microorganism-based-green synthesis was greatly introduced for medical (Zhang *et al.*, 2020) and agriculture (Bahrulolum *et al.*, 2021) applications in the past decades due to

the usage of less toxic chemicals (Augustine *et al.*, 2020). Template synthesis was able to enhance the photocatalytic activity of nanomaterials due to its ability to control the morphology and size of the nanomaterials (Li *et al.*, 2018; Kale *et al.*, 2019).

In this project, a bottom-up synthesis method, known as the DH method, would be introduced for the synthesis of MgO nanomaterials. This synthesis method has advantages such as a simple yet cost-effective process that can produce MgO nanomaterials. Nanomaterials could be formed by applying low heating power and shorter heating duration with a simple set-up. The produced nanomaterials will be grown on the surface of the substrate, which allows a strong contact between the materials and the substrate, thus reducing the chance of peeling off or chipping off during application. MgO nanomaterials were selected for this project because of their good optical properties, ability to degrade toxic dye (Venkata Ratnam *et al.*, 2019; Albouyeh *et al.*, 2020), readily available, and low toxicity (Samadi *et al.*, 2021), which is well suited as photocatalyst for pollutants removal or toxic waste remediation (Fernandes *et al.*, 2020).

1.3 Problem statement

(i) Time-consuming synthesis process

MgO nanomaterials are potential materials to be used as photocatalysts for dye degradation as they have a low refractive index from 1.62 to 1.74 (Zheng *et al.*, 2012), high surface area, and adsorption capacity that improves the dye adsorption ability (Allawi, Juda, and Radhi, 2020). Many research works have been done to synthesize MgO nanomaterials. For example, Jeevanandam *et al.* (2018) synthesized MgO nanorods using Eucalyptus globulus aqueous leaf extract, which is commonly available in Malaysia; Sutapa *et al.* (2018) and Sierra-Fernandez *et al.* (2017) produced MgO nanoparticles using the sol-gel method; Darvishi, Soltani, and Safari (2017) produced MgO

nanomaterials using the ultrasonic assisted method; Cui *et al.* (2014) produced mesoporous MgO nanomaterials using the hydrothermal method; and Kamarulzaman, Chayed, and Badar, (2016) produced MgO nanoparticles using solid-state synthesis method.

These synthesis methods are time-consuming for MgO nanomaterials synthesis. Khan *et al.* (2020) took 4 days to dry the biomaterial under sunlight in dust-free conditions, incise, extra 4 hr to boil and stir, and filter to produce the Dalbergia sissoo plant extraction as the precursor of the Green synthesis approach to produce MgO nanoparticles; Sierra-Fernandez *et al.* (2017) took 24 hr of mixing and 3 hr of annealing for the synthesis of MgO nanoparticles using the sol-gel method; Darvishi, Soltani and Safari, (2017) took at least 24 hr for the synthesis of MgO nanoparticles using the ultrasonic method; Cui *et al.* (2014) needed 6 hr for the synthesis of MgO nanomaterials using hydrothermal method while Chamack, Mahjoub, and Hosseinian, (2018) used 1 hour for the synthesis of MgO nanoparticles; Kamarulzaman, Chayed, and Badar, (2016) used at least 6 hr for the synthesis MgO nanoparticles using solid-state synthesis method.

(ii) The difficulty of large-scale production

The above synthesis methods are not feasible for large-scale production due to the lack of cost-effective large equipment available for them to produce nanomaterials on a large scale. A small size (diameter: 10.60 cm) autoclave reactor for the hydrothermal synthesis method costs about RM 20700.00. An industrial-scale Sonicator for ultrasonic-assisted method costs about RM 71000.00 with a maximum capacity of 20 L (homogenizers.net, 2022) while a microwave used for microwave-assisted synthesis costs RM 11000.00, not to mention that using microwave-assisted synthesis will bring carcinogenic effect to human health due to long term microwave exposure (Yakymenko *et al.*, 2011).

This series of studies indicated that there is still a lack of cost-effective synthesis methods that can produce MgO nanomaterials on a large scale within a short period without affecting human health and have a low wastage of raw materials. The DH method is a potential candidate that suits these requirements.

(iii) Secondary pollutants for the wastewater treatment process

Photocatalysts in particle form tend to lose and carry away by wastewater during its treatment process. This will become problematic due to its effects on human and aquatic life remains unknown. Thus, losing a high amount of photocatalysts, e.g. MgO particles to the wastewater might generate secondary pollutants. Additional treatments will be needed to collect the lost particles. Furthermore, the loss of photocatalysts in the wastewater will significantly reduce the photocatalytic performance over time and require more cost and time to replenish the photocatalysts. To counter this issue, researches have been done to grow photocatalysts on supporting substrates such as ceramic (De Araujo Scharnberg *et al.*, 2020), stainless steel (Zhu *et al.*, 2001), zeolite (Albouyeh *et al.*, 2020), activated carbon (Karimi *et al.*, 2015) and glass (Tlili *et al.*, 2021) and reduce the possibility of losing them. Till now, no research work has been done to produce MgO nanomaterials and to grow them on supporting substrates using the DH method.

This project aims to synthesize MgO nanomaterials on kanthal wires via the DH method. Process optimization was carried out by systematically studying the effects of power supply and the heating time on the growth of MgO nanomaterials on these substrates. The MgO nanomaterials produced by the DH method are expected to have superior performance in the degradation of organic dyes due to their minute size.

1.4 Research Objective

- (i) To set up and synthesize MgO nanomaterials using the DH method.
- (ii) To characterize the structural, optical, and photocatalytic properties (photocatalytic degradation of MB) of MgO nanomaterials that were grown on kanthal wires and MgO particles (by-product).

1.5 Scope of Study

In this project, MgO nanomaterials were synthesized using the DH method. The optimum parameters were determined by studying the effect of heating power, pH value, and heating duration on the growth of MgO nanomaterials on kanthal wires. The MgO nanomaterials grown on the kanthal wires and their by-products were characterized using X-ray Diffraction (XRD), Fourier transform infrared spectrometer (FTIR), UV-Vis spectroscope, Field Emission Scanning Electron Microscope (FESEM) & Energy Dispersive X-ray (EDX), and Transmission Electron Microscope (TEM). The photocatalytic performances of MgO nanomaterials were tested using methylene blue (MB) under UV light irradiation. Scavenger tests were used to determine the reactive species presented in the degradation of MB dye.

1.6 Thesis Outline

This thesis comprises 5 chapters.

Chapter 1 introduces the research background, problem statement, research objectives, and the scope of the study.

Chapter 2 presents the literature review of MgO, the synthesis methods used to produce MgO nanomaterials, the classification of dye, the details of MB dye, and the general degradation mechanism of dyes using photocatalysts.

Chapter 3 denotes the methodology of this study. This chapter discusses the material, equipment, synthesis method, and characterization methods used in this study.

Chapter 4 presents the results, analyses, and discussion. The suitability of the DH method to synthesize MgO nanomaterials would be systematically studied.

Chapter 5 concludes the findings of this project with recommendations for future studies.

CHAPTER 2 LITERATURE REVIEW

2.1 Introduction

This chapter reviews the crystal structures and optical properties of MgO in bulk and nano size. MgO nanomaterials possess good optical properties for instance relatively low refractive index and low band gap as compared to MgO in bulk. These properties open the opportunity for MgO nanomaterials to be used as photocatalysts. Researchers also stated that MgO could be used for heavy metal adsorption, magnetic sensors, and antibacterial agent (Cao *et al.*, 2012; Rao *et al.*, 2013; Salehifar *et al.*, 2016; Podder *et al.*, 2018; Sackey *et al.*, 2020a). This chapter also presents several types of MgO nanomaterials, and synthesis methods as well as their advantages and disadvantages that have been reported by researchers. Subsequently, the potential applications of MgO nanomaterials, particularly as the photocatalyst, will be discussed. The crucial factors that affect the photocatalytic performances of photocatalysts, photodegradation mechanism, and scavenger test will be presented. Lastly, the classification of dye which includes ionic and non-ionic and MB dye specifically will be described in detail.

2.2 Magnesium Oxide (MgO)

Magnesium oxide (MgO) is an ionic material that consist of Mg^{2+} ions and O^{2-} ions in $1s^22s^22p^6$ and $1s^22s^22p^6$ configuration respectively with empty d-orbitals. MgO belongs to the periclase group which has a rock-salt structure in nature as shown in Figure 2.1. It also belongs to the metal oxide group which is well-suited for sensors, bio-imaging detectors, optical devices, antibacterial, and wastewater applications due to the presence of cations with valence states and anions with deficiencies that causes carriers depletion (Gangwar *et al.*, 2016).

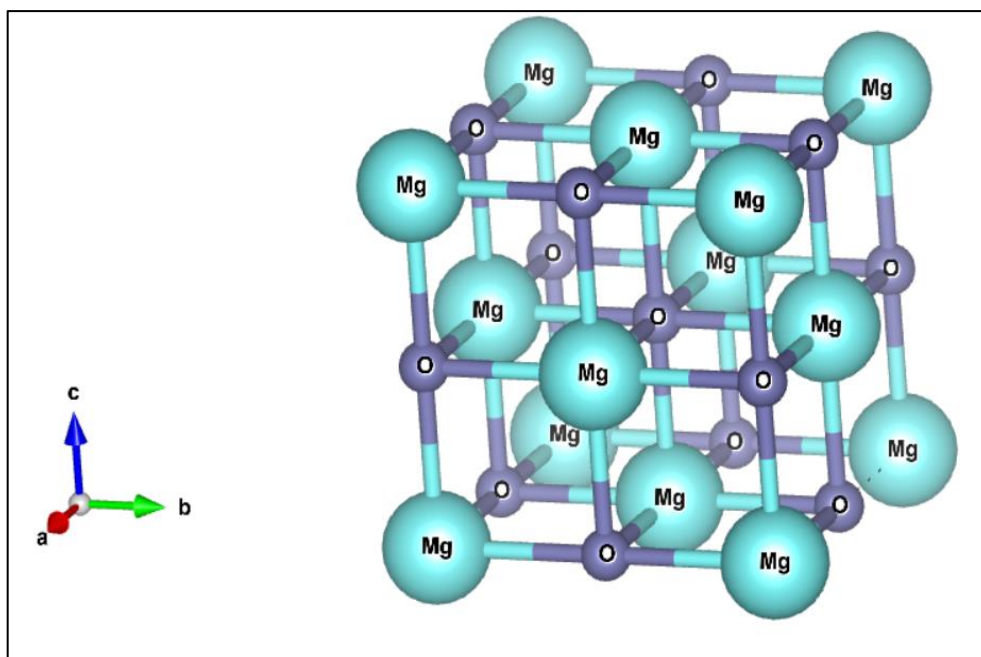


Figure 2.1: Crystal structure of MgO (Smyth *et al.*, 2000).

Bulk MgO has many unique properties. It is a wide bandgap semiconductor of 7.77 eV (Nourozi *et al.*, 2019), with great thermodynamical stability with enthalpy of formation of -601.5 kJ/mol (Putnis, 2012), low refractive index from 1.62 to 1.74 (Zheng *et al.*, 2012), low dielectric constant from 3.2 to 9.8 with dielectric loss of approximately 10^{-4} at ambient temperature under 1 MHz frequency condition (Hornak *et al.*, 2018). Nevertheless, some of these properties change significantly in nanosize. For instance, Nemade and Waghuley (2014) reported that the band gap of MgO nanoparticles produced via solvent-mixed spray pyrolysis was 4.2 eV instead; Badar *et al.*, (2012) also reported that the band gap of MgO nanoparticles produced by the sol-gel method was in the range of 5 to 6 eV. It was also reported that the refractive index of MgO nanoparticles was in the range of 1.008 to 1.026 (Nemade *et al.*, 2014).

The wide band gap of bulk MgO (~7.8 eV) might give a wrong perception that it is not suitable to be used as a photocatalyst. High energy light source with a wavelength smaller than 159 nm is needed to excite MgO to produce photo-generated electrons and

holes. Nevertheless, MgO nanomaterials demonstrated good photocatalytic activity (Hai *et al.*, 2017). UV irradiation and sunlight exposure provides photo energy for the hydroxyl radicals formation in photocatalytic degradation process. The photon also causes excitation of the electron in the conduction band, and jump to the defect's site/ valance band, leaving holes in the conduction band. The holes existed will reacts with water, thus producing more hydroxyl radicals for the photocatalytic degradation process. According to Hai *et al.*, the MgO nanomaterials have a narrower band gap as compared to bulk materials and they contained high surface defects. Therefore, MgO nanomaterials were synthesized by the DH method, and its potential as a photocatalyst to degrade methylene blue was studied.

2.3 Synthesis methods of MgO nanomaterials

Various synthesis methods such as sol-gel (Sierra-Fernandez *et al.*, 2017; Sutapa *et al.*, 2018), ultrasonic (Darvishi *et al.*, 2017), hydrothermal (Cui *et al.*, 2014; Dhal *et al.*, 2015), green (Jeevanandam *et al.*, 2018), microwave-assisted (Selvam *et al.*, 2011a; Jeevanandam *et al.*, 2018), and solid-state synthesis (Kamarulzaman *et al.*, 2016; Chamack *et al.*, 2018) have been developed to obtain MgO nanomaterials.

2.3.1 Sol-gel method

A sol-gel method is a well-known approach to forming nanoparticles. Generally, synthesizing MgO nanomaterials via the sol-gel method requires a water-soluble Mg salt mixed with an appropriate organic host. After vigorous stirring, the mixture will form sol whereby formation of colloidal particles via hydrolysis reaction. Mixing and stirring help to convert the solution, 'sol' into 'gel' via a condensation reaction. Heating the 'gel' helps to form the precursor and annealing of the precursor will then form MgO nanomaterials. Figure 2.2 shows the steps involved in the sol-gel method.

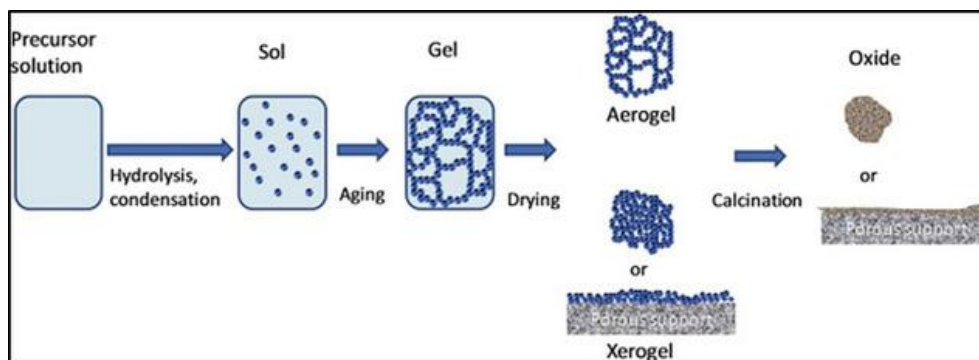


Figure 2.2: Steps involved in the sol-gel method (Kallawar *et al.*, 2021).

According to Sutapa *et al.* (2018), MgO nanoparticles with an average size of 7.51 nm were successfully obtained via the sol-gel method with magnesium acetate and oxalate to form Mg-oxalate precursor at pH 5 conditions as shown in Figure 2.3. Methanol was used to dissolve the Mg-oxalate precursors, followed by annealing at 500 °C for 6 hr. Similarly, Sierra-Fernandez *et al.* (2017) successfully produced MgO nanoparticles with an average size of 19.6 nm by using magnesium ethoxide and sodium hydroxide via the same method. The two solutions were mixed and stirred for 24 hr, followed by centrifugation and washing with distilled water and ethanol. The samples were then dried and annealed at 650 °C for 3 hr.

The advantages of the sol-gel method are high purity, narrow size distribution and homogeneity of product, cost-effectiveness process, and relatively simple process (Mastuli *et al.*, 2014). On the downside, the cost for the raw materials is somewhat higher; the processing time for the sol-gel method is longer (more than 6 hr) and the organic solvent used for the precursor solution can be toxic (Modan and Plăiașu, 2020).

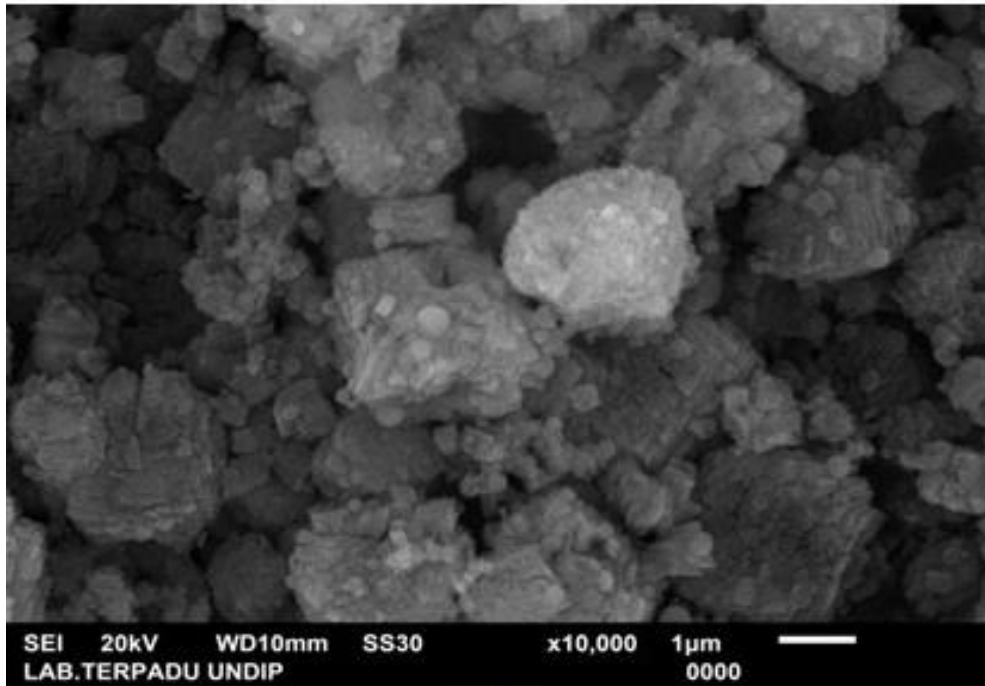


Figure 2.3: SEM micrograph of MgO nanoparticles produced by Sutapa et al. (2018).

2.3.2 Ultrasonic method

The ultrasonic method utilizes ultrasound to assist nanomaterials synthesis in an aqueous solution (Gedanken, 2004). Ultrasound is a soundwave that ranges from 20 kHz to 10 MHz. In this process, ultrasound is irradiated to the solution, causing the solution to gain a high amount of energy, and allowing chemical reactions. The high energy is mainly caused by the cavitation process. Cavitation happens when the applied ultrasound causes continuous cyclic in high and low-pressure conditions in the solution whereby the low-pressure state helps to grow the bubbles while the high-pressure state helps the bubble to grow until its extreme size becomes unstable and collapses. Upon the bubble collapse, it will obtain a very high temperature and thus able to break chemical bonds. Therefore, this continuous process of creating, growing, and collapsing produces a high amount of energy and allows chemical reactions to produce nanomaterials (Gedanken, 2004; Karimi *et al.*, 2021).

To form MgO nanomaterials via the ultrasonic method, water-soluble magnesium salt is required as a precursor and mixed with a basic chemical reagent (usually sodium hydroxide), which acts as a precipitant. According to Darvishi, Soltani, and Safari, (2017), MgO nanomaterials could be obtained via the ultrasonic method with magnesium nitrate hexahydrate as the precursor and sodium hydroxide to be added dropwise under stirring in an ultrasonic bath for 120 min. Then, the suspension was washed and dried for 24 hr. MgO nanomaterials could also be formed by using magnesium acetate monohydrate as a precursor and hydrochloric acid to be added dropwise under vigorous stirring conditions. The stirred solution was sonicated for 30 min, followed by heating from room temperature to 130 °C with continuous sonication. The sample was collected and washed, followed by air drying for 48 hr. This has been done by Gandhi *et al.* (2011) and rod-like structures of MgO nanomaterials were formed as shown in Figure 2.4.

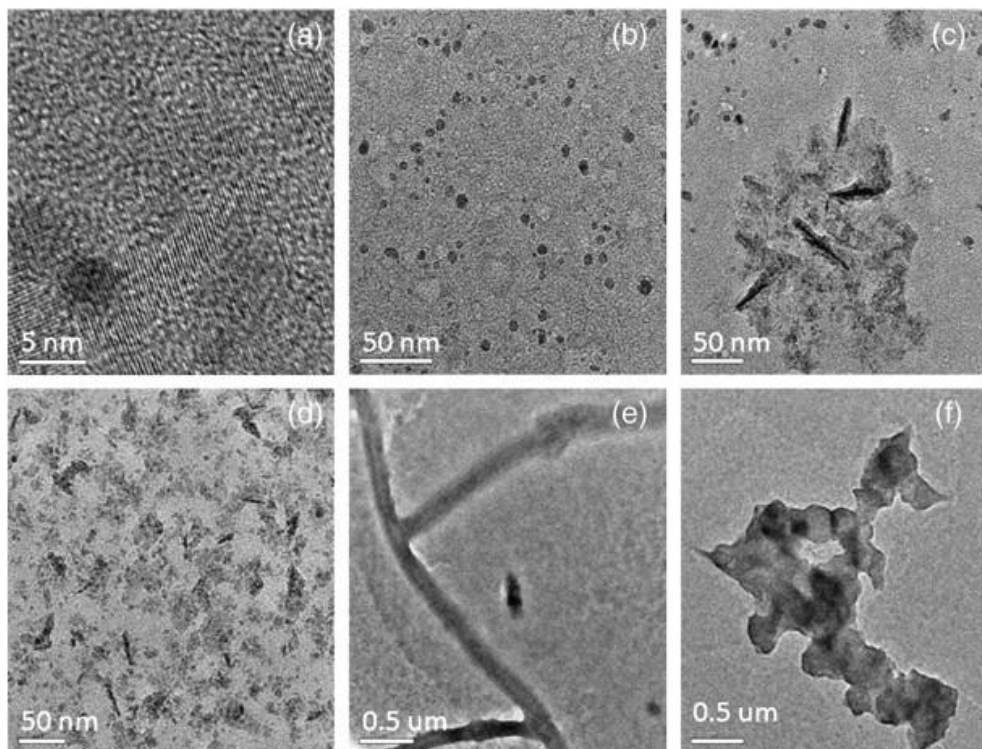


Figure 2.4: HRTEM micrograph of MgO nanomaterials formed by Gandhi *et al.* (2011).

The advantages of this method are improved chemical reaction rate for the synthesis, products can be formed without the need for additives, and it also requires fewer reaction steps to form the desired product (Modan and Plăiașu, 2020). In contrast, deciding the optimum conditions and parameters in this method is a major challenge as this will affect the cavitation mechanism and the resulting product. In addition, it is not available for large-scale production due to the less availability of large equipment that can produce nanomaterials using the ultrasonic method (Ramirez-Corredores, 2017).

2.3.3 Hydrothermal method

The hydrothermal method is a solution-based route for nanomaterials synthesis. It involves a mixing process between the precursors with an appropriate chemical reagent that helps to obtain a crystalline nanomaterial. The mixture will then be transferred to a closed vessel and heated with a temperature of above 100 °C, pressure above 1 bar, and time (Ng *et al.*, 2020). The closed vessel facilitates the chemical reaction of the precursors (Qiu *et al.*, 2021). The hydrothermal method is a one-step process that utilizes the synergistic effect of high temperature and pressure (Huang *et al.*, 2018).

According to Cui *et al.* (2014), the uniform morphology of mesoporous MgO was formed via the hydrothermal method with magnesium nitrate hexahydrate as the precursor, mixed with dropwise sodium carbonate solution. The solution was sealed and heated to different temperatures and times for characterization. The result stated that a lower heating temperature (160 °C) and a longer heating time (24 hr) resulted in a finer size of MgO nanomaterials (9.5 nm pore diameter). On the other hand, Dhal *et al.* (2015) successfully produced MgO nanoflakes as shown in Figure 2.5 with an average diameter of 400 nm. Magnesium chloride hexahydrate and ammonium carbonate solution were used as the precursor and underwent hydrothermal treatment at 150 °C for 6 hr. Then, the solution was washed, dried, and calcined at 400 °C for 3 hr.

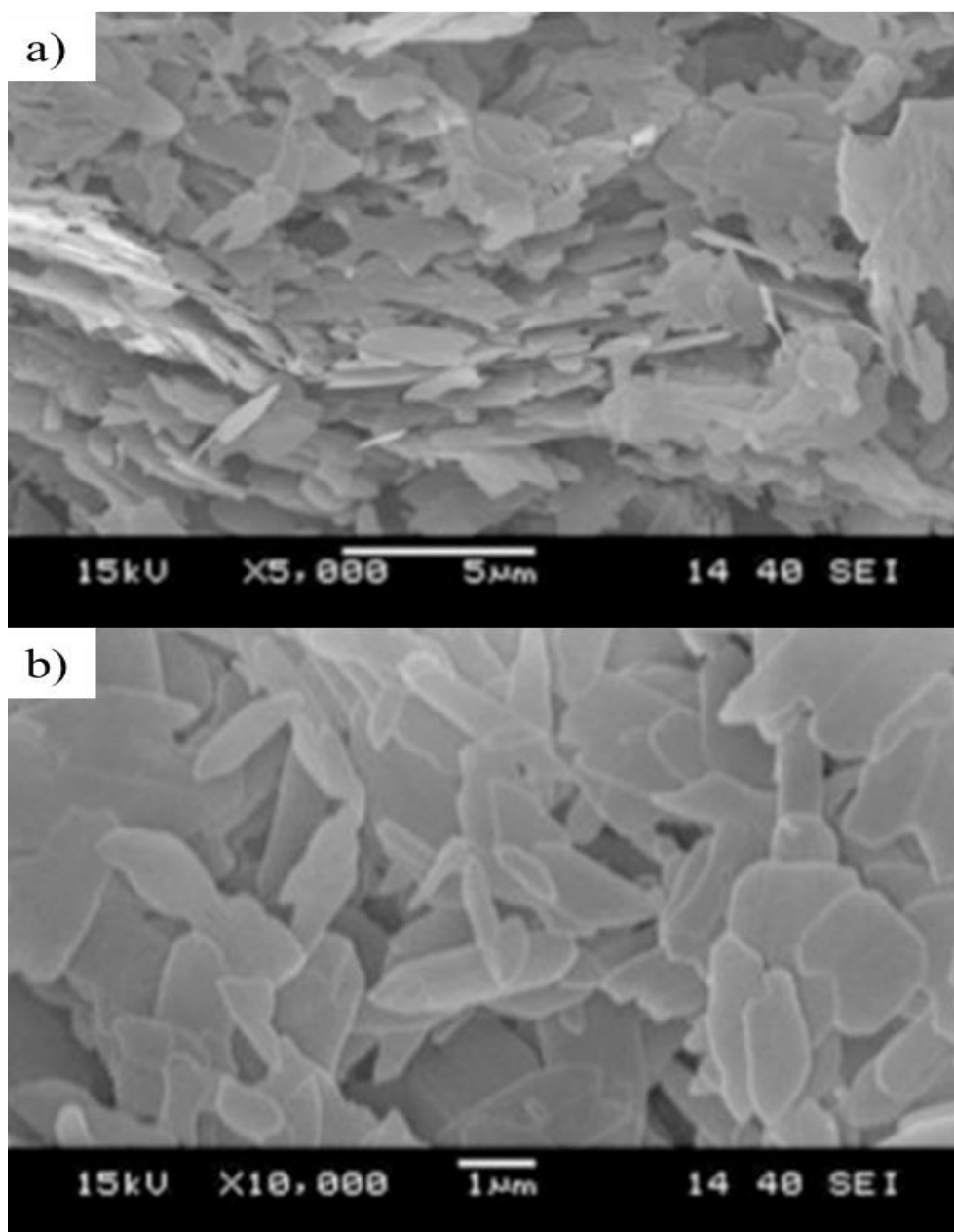


Figure 2.5: SEM images of MgO nanoflakes produced by Dhal et al. (2015) observed under magnification of (a) 5,000 X and (b) 10,000 X.

The advantages of the hydrothermal method are improved chemical reactivity of the precursors, can easily formation of metastable state products, and precise control of the size and shape of the product. The disadvantage of using this synthesis method is the expensive apparatus, i.e. the closed vessels (usually autoclaves). The process may have safety issues during the reaction due to high pressure and temperature, and it is not available to observe the process in closed vessels (Ahmadi *et al.*, 2014).

2.3.4 Green synthesis

Green synthesis is a method that produces nanomaterials by precursors mixed with biological extracts that can act as reducing, capping, solving, or stabilizing agents. Specific bacteria can be used as a reducing agent for reducing Mg salts to form MgO nanomaterials. The micro-organism undergoes an extracellular mechanism to secrete enzymes and proteins for the reduction process and acts as a stabilizer simultaneously. Next, fungi can be used as a reducing agent in nanomaterial synthesis as it undergoes the same mechanism as bacteria. Moreover, plant extracts can act as stabilizers, reducing agents and neutralizing reactive oxygen species in nanomaterials synthesis (Abinaya *et al.*, 2021). Jeevanandam, Chan and Ku (2018) have successfully synthesized MgO nanorods and nanoparticles via green synthesis and One-factor-at-a-time (OFAT) approach with magnesium nitrate hexahydrate as the precursor mixed with dropwise Eucalyptus globulus aqueous leaf extract as reducing agent and stabilizer at 80°C under stirring condition. The result showed that 20 min of reaction time resulted in 43.82 nm of particle size.

Green synthesis is more environmentally friendly as less toxic chemicals will be used, economical, higher yield, and convenient (Abinaya *et al.*, 2021). On the contrary, this method is time-consuming as time is required to clean or remove the impurities on the material for instance plant, and to obtain a biological extract or to culture the micro-

organisms. Next, specific parameters such as temperature and pressure are needed to ensure the reaction for the precursors to occur (Garibo *et al.*, 2020).

2.3.5 Microwave-assisted method

The microwave-assisted synthesis is a method that utilizes microwave irradiation which ranges between 0.3 GHz to 300 GHz, to transfer energy directly via dipolar polarization and ionic conduction mechanism to the precursor solution, resulting in rapid and homogeneous heating of the solution (Zhu *et al.*, 2014). Producing Mg nanomaterials requires magnesium salt as a precursor and an organic solvent or an aqueous medium that acts as a reducing agent (Saleh *et al.*, 2017).

According to Mirzaei and Davoodnia (2012), MgO nanoparticles were formed via microwave-assisted sol-gel synthesis at 350 W and pH 10.5 conditions for 15 min with magnesium hydroxide gels in aqueous solution as precursor and ammonia solution as precipitant. The precipitate was then cooled, and dried for 1 hour, followed by calcination for 2 hr at 500 °C. The resulting MgO nanoparticles are with an average particle size of 10.0 nm as shown in Figure 2.6. According to Selvam *et al.*(2011), MgO nanosheets with 20 – 30 nm thickness could be formed via microwave-assisted combustion method with magnesium nitrate mixing with urea under 15 min stirring and followed by heating in a microwave oven at 750 W for 10 min. The solution then reached the spontaneous combustion point which vaporized the solution and turned it into solid. The solid was washed and dried for 2 hr subsequently.

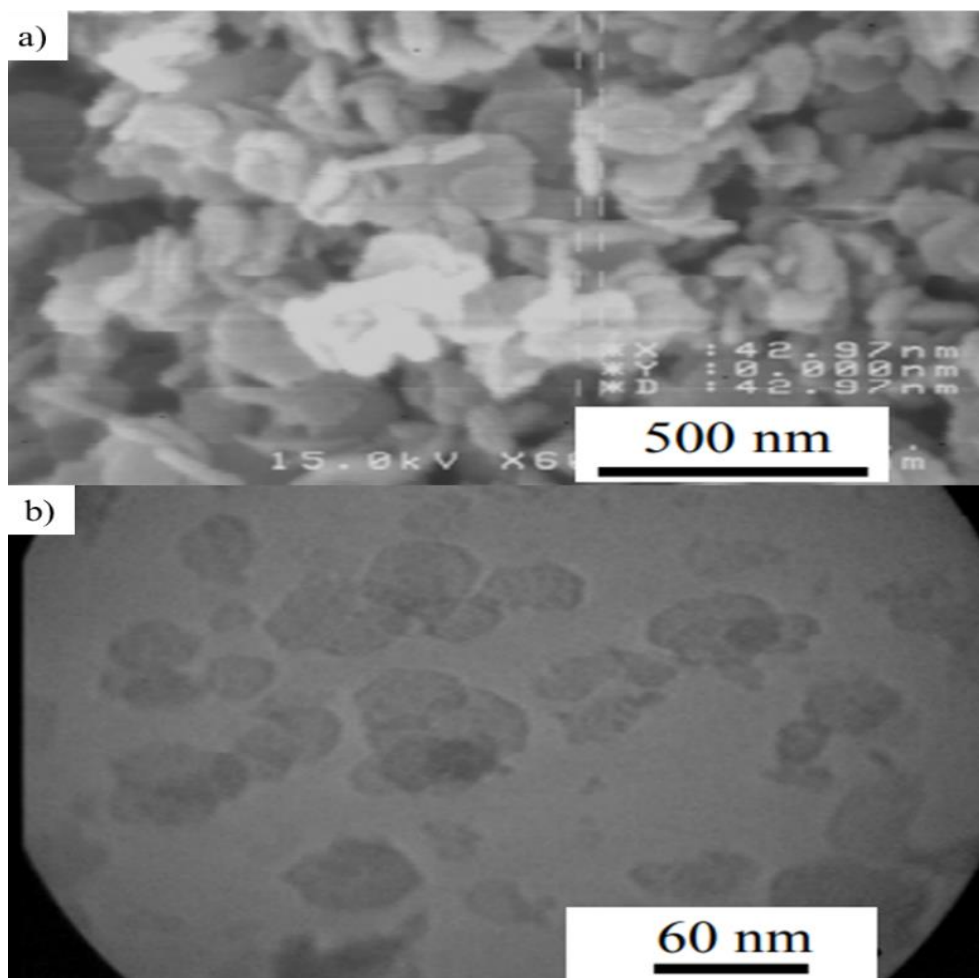


Figure 2.6: (a) SEM (b) TEM micrograph of MgO nanoparticles synthesized using the microwave-assisted method by Mirzaei and Davoodnia (2012).

The advantages of this method are that the product's shape and size could be controlled easily via instrument or parameters tuning, have more uniform heating, and thus obtain a product with good homogeneity, and the reaction rate to form the product is enhanced by the presence of microwave. Conversely, the disadvantages of this method are there are few or limited materials available that can absorb microwaves and occur reaction, unable to produce in large scale basic whereby the batch size is typically limited to a few grams. It might have health hazards for long-term users due to the usage of microwaves in this method (Saleh *et al.*, 2017).

2.3.6 Solid-state synthesis

Solid-state synthesis is a method to produce nanomaterials via solventless reaction without using any liquid media (Chamack *et al.*, 2018). In this method, the product is obtained via the mechanochemical reaction between precursor powders in a solid state (Jamal *et al.*, 2013). Generally, to obtain MgO nanomaterials, magnesium salts would be used as precursors with the addition of appropriate chemical reagents or sodium halide salts as morphology modifiers.

According to Chamack, Mahjoub, and Hosseinian (2018), MgO nanoparticles were successfully formed by crushing magnesium chloride hexahydrate, sodium hydroxide, and sodium bromide precursors followed by heating in a closed furnace at 500 °C for an hour. The MgO nanoparticles had particle sizes in the range of 30 to 50 nm. On the other hand, Kamarulzaman, Chayed, and Badar, (2016) synthesized MgO nanoparticles with particle sizes in the range of 20 to 135 nm by grounding magnesium acetate tetrahydrate, followed by annealing at 800 °C for 6 hr, 12 hr, and 24 hr. Figure 2.7 shows the FESEM micrograph after annealing for 6, 12, and 24 hr.